Volcanoes of the Diamante cross-chain: evidence for a mid-crustal felsic magma body beneath the Southern Izu–Bonin–Mariana arc

ROBERT J. STERN[1]*, YOSHI TAMURA[2], OSAMU ISHIZUKA[3], HIROSHI SHUKANO[2], SHERMAN H. BLOOMER[4], ROBERT W. EMBLEY[5], MATTHEW LEYBOURNE[6], HIROSHI KAWABATA[2], AKIKO NUNOKAWA[2], ALEXANDER R. L. NICHOLS[2], EDWARD KOHUT[7] & IGNACIO PUJANA[1]

[1]*Geosciences Department, University of Texas at Dallas, Box 830688, Richardson, TX 75083-0688, USA*

[2]*Institute for Research on Earth Evolution (IFREE), Japan Agency for Marine-Earth Science and Technology (JAMSTEC), Yokosuka 237-0061, Japan*

[3]*Institute of Geoscience, Geological Survey of Japan/AIST, Tsukuba 305-8567, Japan*

[4]*Department of Geosciences, Oregon State University, 128 Kidder Hall, Corvallis, OR 97331, USA*

[5]*Pacific Marine Environmental Laboratory/NOAA, Newport, OR 97365-5258, USA*

[6]*ALS Geochemistry, 2103 Dollarton Hwy, North Vancouver, BC Canada V7H 0A7*

[7]*Department of Geological Sciences, University of Delaware, Newark, DE 19716, USA*

**Corresponding author (e-mail: rjstern@utdallas.edu)*

Abstract: Three submarine Diamante cross-chain volcanoes in the southern Mariana arc mark a magma-healed zone of along-arc (north–south) extension that allows either mafic mantle-derived basalts or felsic magmas from the middle of thickened arc crust to erupt. The largest volcano is East Diamante, with a well-developed (5 × 10 km) caldera that formed via violent felsic submarine eruptions beginning nearly 0.5 Ma. One or more of these eruptions also formed a giant submarine dune field extending 30 km to the NW of the volcano. Felsic igneous activity continues at least as recently as *c.* 20 000 years ago, with emplacement of resurgent dacite domes, some hot enough to power the only black smoker hydrothermal system known in the Mariana arc. In contrast, felsic eruptions do not occur on the two volcanoes to the west, implying that the mid-crustal felsic zone does not underlie the thinner crust of the Mariana Trough back-arc basin. Diamante cross-chain lavas define a medium K suite; mafic lava phenocryst assemblages show arc-like associations of anorthite-rich plagioclase with Fe-rich olivine. Magmatic temperatures for a basaltic andesite and three dacites are *c.* 1100 °C and *c.* 800 °C, respectively, typical for cool, wet, subduction-related felsic magmas. Felsic magmas formed under low-P crustal conditions. The Diamante cross-chain is the southernmost of at least seven and perhaps eight Mariana arc volcanoes in a *c.* 115 km long arc segment characterized by felsic eruptions. This is the 'Anatahan Felsic Province', which may have formed above a mid-crustal tonalite body that formed by fractionation or was re-melted when heated by *c.* 1200 °C mafic, mantle-derived magmas. Across- and along-arc variations suggest that felsic eruptions and dome emplacement occurred when midcrustal tonalite was remobilized by intrusions of mafic magma, while north–south extension facilitated the development of conduits to the surface.

Supplementary material: Detailed Hyperdolphin ROV dive tracks, Cook 7 dredge locations, $^{40}Ar/^{39}Ar$ analytical data, analytical methods, major and selected trace element analyses of whole rock samples, and compositional data for minerals are available at http://www.geolsoc.org.uk/SUP18611

The Izu–Bonin–Mariana arc system (IBM) extends over 2800 km south from near Tokyo, Japan, to beyond Guam, USA (Fig. 1a), and is an excellent example of an intra-oceanic arc system (IOAS; Stern 2010). IOASs are built on oceanic crust and contrast in several ways with arcs built on continental crust, such as Japan or the Andes. Because IOAS crust is thinner, denser and more refractory than that beneath Andean- or Japan-type margins, study of IOAS melts and fluids allows more confident

From: Gómez-Tuena, A., Straub, S. M. & Zellmer, G. F. (eds) 2014. *Orogenic Andesites and Crustal Growth*. Geological Society, London, Special Publications, **385**, 235–255.
First published online June 27, 2013, http://dx.doi.org/10.1144/SP385.6

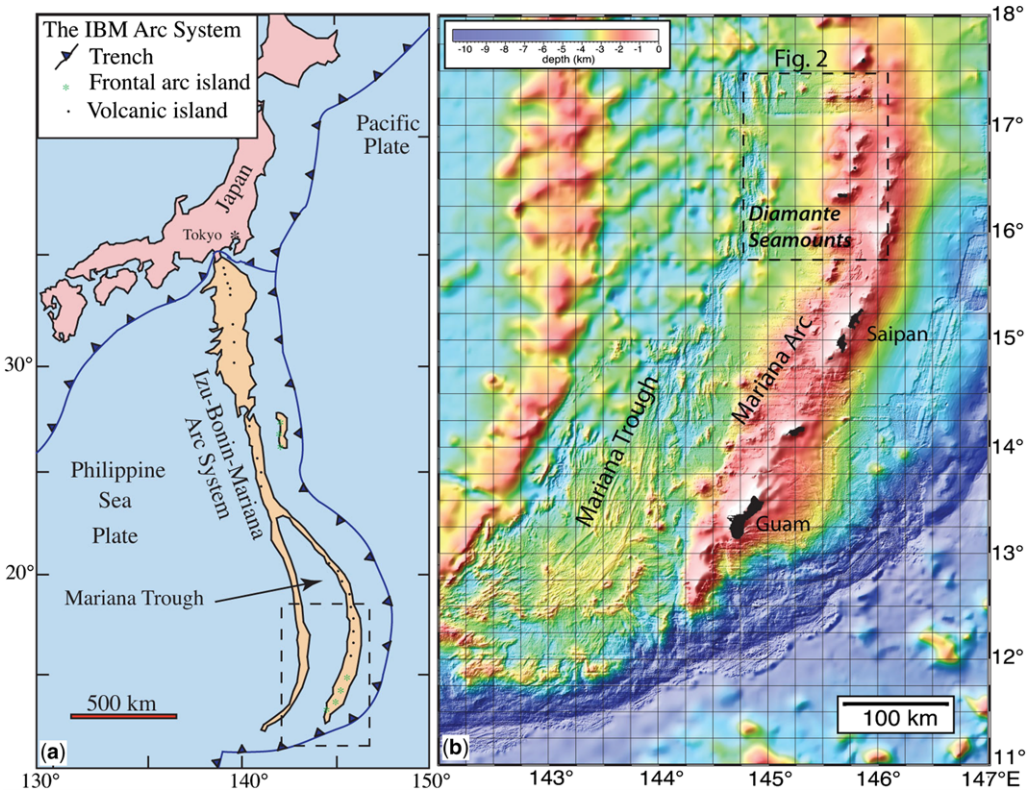

Fig. 1. Locality maps. (**a**) The Izu–Bonin–Mariana arc system in the western Pacific, dashed box shows the location of (b). (**b**) The southern Mariana arc system, showing the area of Figure 2 in dashed box.

assessment of mantle-to-crust fluxes and processes than is possible for continental arcs. We are particularly interested in understanding felsic IOAS rocks better because the latter are microcosms of continental crust formation that must be generated by fractionation or melting of mafic arc crust. The IBM arc system is an excellent natural laboratory for studying these rocks, because felsic rocks are common, even though basalt and basaltic andesite ($<$57 wt% SiO_2) are clearly the predominant eruptive products (Tamura & Tatsumi 2002; Straub 2008). In this contribution, we advance our understanding of IOAS felsic magmagenesis by describing a new occurrence of these rocks in the southern Mariana arc (Fig. 1b) and explore several interesting aspects of these rocks.

The Mariana arc system shows important along-strike variations in tectonic and magmatic behaviour, including the fact that arc volcanism south of Anatahan (Fig. 2) is entirely submarine (Stern *et al.* 2003). A distinctive east–west-trending set of three volcanoes was first investigated during the 1979 Mariana expedition by Dixon & Stern (1983), who named the seamounts in consonance with other nearby Mariana arc seamounts, Esmeralda and Ruby. Over the past decade, southern Mariana submarine volcanoes have become foci of increasingly detailed studies. During the Cook 7 expedition in 2001 aboard R/V *Melville,* this region was bathymetrically mapped and surveyed with HAWAII MR-1 towed sonar and extensively dredge-sampled, including several dredges around the study area, the Diamante cross-chain. In 2003 and 2004, a NOAA team investigated submarine hydrothermal activity in the Mariana arc, including seafloor studies using the Canadian ROV ROPOS. The many discoveries during the NOAA cruises included an extensive, vigorous hydrothermal field in the caldera of East Diamante (Baker *et al.* 2008). Japanese and US scientists, using the JAMSTEC ROV *Hyper-Dolphin* aboard the R/V *Natsushima* (NT09–08, June 2009), began studying the Diamante cross-chain during eight dives (HPD1011–1018), returning to the study area in 2010 during NT10–12.

The study area is of particular petrological interest because it is part of a 115 km-long Mariana arc segment characterized by felsic volcanism (Fig. 2; Stern & Hargrove 2003). Seven edifices within

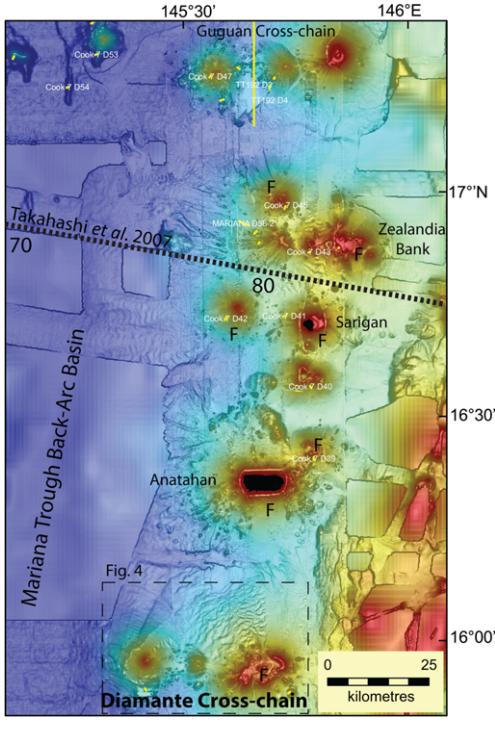

Fig. 2. Anatahan felsic province of the Mariana arc showing the location of the Diamante cross-chain. 'F' indicates volcano with felsic (>60 wt% SiO_2) lavas. Short dashed line 'Takahashi *et al.* 2007' is deep seismic profile of Takahashi *et al.* (2007), summarized in Figure 3. '70' and '80' are OBS locations. Dashed box shows location of detailed study area in Figure 4.

this region, including the 2003 Anatahan eruption (Wade *et al.* 2005), have erupted felsic lavas. Volcano size – proxy for age and, hence, the presence of evolved magmatic storage systems – does not seem important in controlling the concentration of felsic eruptions within this segment. Instead, felsic magmas may be tapped from a 3–5 km thick 'tonalite layer' in the mid-crust, with V_p = 6.1–6.5 km s^{-1}, beneath the volcanic front edifices (Fig. 3; Takahashi *et al.* 2007). This layer tapers away to the west, where rear-arc cross-chain volcanoes erupting only basalts are found. Crustal structure beneath the volcanic front edifices has also been studied by Calvert *et al.* (2008). These studies show that the middle crust is thickest beneath volcanic front edifices.

This report focuses on the results from Cook 7 dredges, ROPOS diving during TT-167, and NT09–08 and NT10–12 *Hyper-Dolphin* ROV dives, with an emphasis on characterizing the distribution of mafic and felsic igneous rocks and presenting a broad petrological outline based on new major element and limited trace element geochemical data. Sixteen dredge or ROV samplings over a 10 × 35 km area provide information on Diamante cross-chain volcanic rocks. Sampling locations are shown on Figure 4 and individual ROV dive tracks with sampling localities are provided in the Supplementary material. A subsequent report will focus on more complete trace element and isotopic data for these lavas and investigate their petrogenesis in more detail.

Submarine volcanoes of the Diamante cross-chain

Three principal volcanoes 10–15 km apart make up the Diamante cross-chain: East Diamante, Central Diamante and West Diamante (Fig. 4). East Diamante marks the Mariana arc volcanic front and lies about 145 km above the subducted slab (Syracuse & Abers 2006). A small volcano sampled by Cook 7 D34 (SE Diamante) lies *c.* 135 km above the slab. Central Diamante lies *c.* 180 km and West Diamante lies *c.* 250 km above the subducted slab. Locations for samplings are shown in Figure 5 and detailed charts for individual dives can be found in the Supplementary material. Details of Cook 7 dredges can also be found in the Supplementary material. These results allow us to sketch the geology of these three volcanoes, at least in broad strokes (Fig. 4).

West and Central Diamante are relatively simple basaltic volcanoes. Our dive results on these volcanoes (HPD1016 and HPD1018, respectively) and the parasitic cone on the eastern slope of West Diamante (HPD1017) are consistent with previous results from dredging during the MARA and Cook 7 expeditions indicating that these are mostly basaltic edifices. Central Diamante is the site of a 2003 earthquake swarm, which Heeszel *et al.* (2008) concluded was due to faulting along an east–west-striking, steeply dipping normal fault plane, with a dominantly N–S-oriented tension axis. Normal faulting is also expressed morphologically at Central Diamante, where east–west-trending normal faults with scarps facing the summit region indicate that this volcano formed over a zone of strong north–south extension. The east–west orientation of the Diamante cross-chain and the similar elongation of East Diamante volcano are also consistent with formation of the cross-chain in a region dominated by north–south extension.

East Diamante is complex, both volcanologically and petrologically. It is also the only Mariana arc volcano known to have a vigorous 'smoker' hydrothermal system (Baker *et al.* 2008), so understanding its geological and petrological evolution is of special interest. Figure 5 depicts

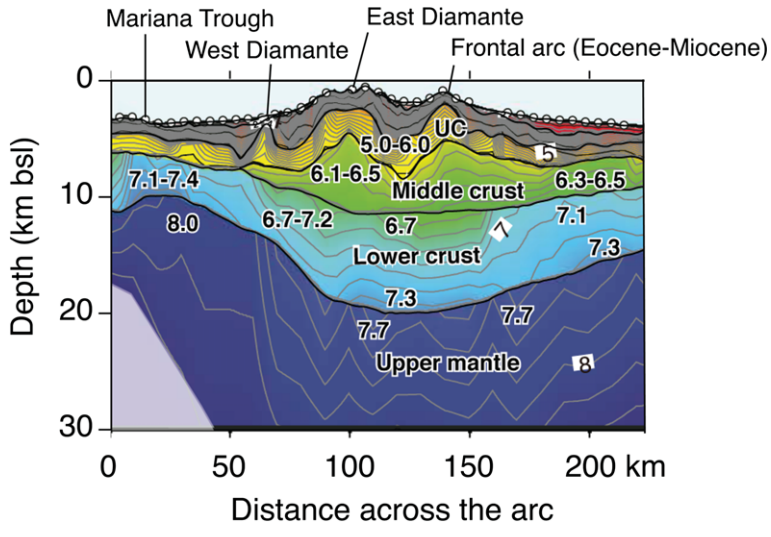

Fig. 3. Crustal structure beneath southern Mariana arc from seismic profile of Takahashi *et al.* (2007). Location of profile is shown on Figure 2; this has been modified to show approximate relative positions of East Diamante and West Diamante volcanoes. Note presence of thick low-V_p layer beneath the volcanic front; this probably also underlies East Diamante.

the summit region of East Diamante volcano, which has the form of a complex caldera, *c.* 10 × 5 km, elongated ENE–WSW and breached on its northern and southwestern sides. The caldera floor is irregular, with several resurgent domes in the middle of the caldera; some of these host hydrothermal activity. The NE caldera wall is the simplest, with a steep inner wall, gentler outer slope,

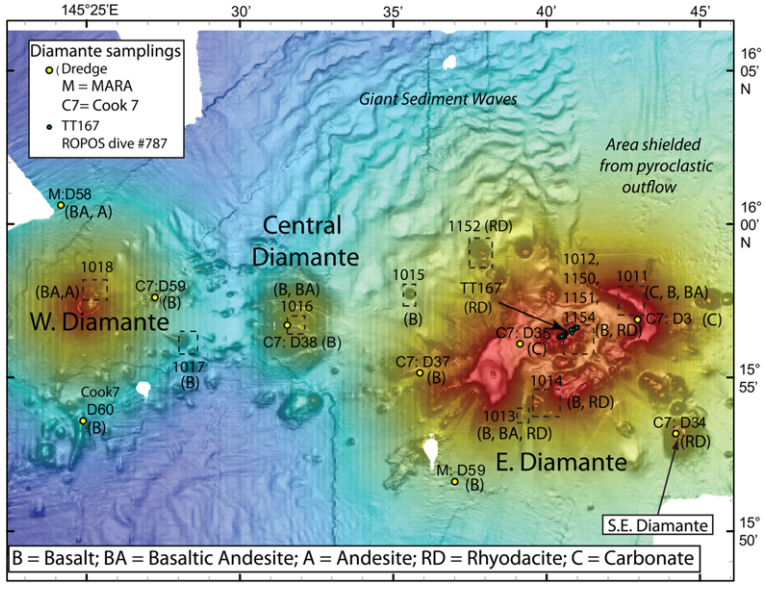

Fig. 4. The Diamante cross-chain, showing the location of Hyperdolphin dives 1011–1018. Detailed maps for each dive are shown in the Supplementary material. Also shown are the locations of previous samplings: MARA dredges 58 and 59 (Dixon & Stern 1983); Cook 7 dredges 34, 37, 38, 59 and 60; and TT167 ROPOS dive 787. Compositions of samples are also indicated.

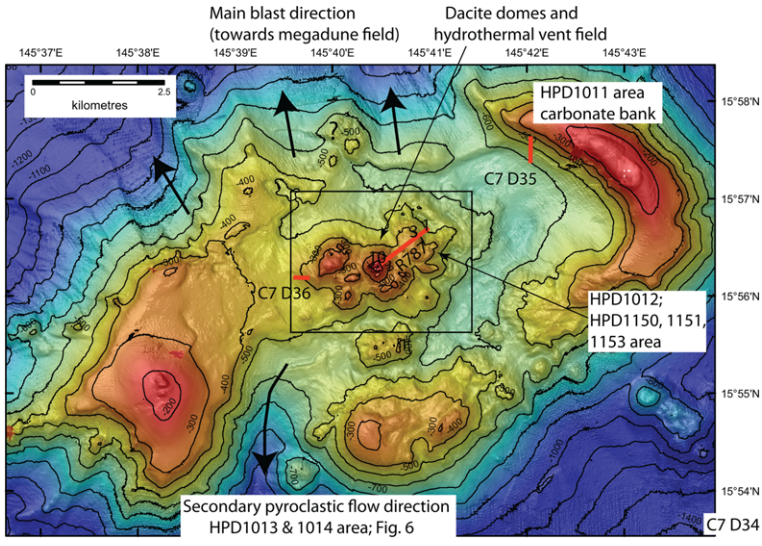

Fig. 5. Bathymetric map of East Diamante volcano, showing general location of 4 Hyperdolphin dives (detailed locations shown in the Supplementary material), Cook 7 dredges D34–D36 (red lines except for D34 which is slightly off the map), and major geological features. Approximate path of TT167 R787 and locations of samples 1, 3 and 10 are also shown.

and a boomerang-shaped outline. This is the only sector of the volcano that is so regular, and we thought before sampling it during Cook 7 D35 and HPD1011 that it would expose pre-caldera collapse volcanic stratigraphy. Results of one dredge and two ROV transects demonstrate that the *c.* 400 m thick section exposed in this scarp is composed of biogenic carbonate sediments and shelly detritus (with a few lavas, apparently interbedded, near the top). Biostratigraphic studies of these carbonates indicate that these are shallow-water deposits of Plio-Pleistocene age. Similar material was recovered from the region west of the resurgent domes in the caldera Cook 7 D36 (Fig. 5; Supplementary material). Because horizontal bedding is exposed in near-vertical exposures – probably associated with faulting accompanying caldera formation – this carbonate sequence probably predates caldera formation. The entire NE sector of the volcano as far south as the morphological change near 15°56′N (from high, steep and smooth to low, gentle and rough) is composed of carbonate rocks. The thickness of these carbonates and paucity of volcanic material indicate that the volcano experienced a significant period of quiescence and subsidence marked by the growth of the carbonate platform. Magmatic resurgence of the volcano culminating in caldera collapse may be indicated by the mafic lavas recovered near the top of the NE caldera wall during HPD1011. We wonder if the unsampled broad, smooth, high west of the caldera might also be dominated by pre-caldera carbonate rocks, but a dredge just to the west of Figure 5 (Cook 7 D37; Supplementary material) recovered pumice, basalts and Mn crust and no carbonate sediments.

Caldera formation marked an important episode of magmatic resurgence of East Diamante. Dive results from HPD1013 in the SW breach provide our best perspective on felsic eruptions from East Diamante caldera. This dive traversed a downcut section of several submarine pyroclastic flows (Fig. 5). Figure 6 is a simplified section based on observations during HPD1013. The *c.* 150 m thick section of felsic pyroclastics and lapilli- and ash-sized is characterized by two *c.* 30 m thick units of coarse pumice breccia separated by finer ash, suggesting at least two violent felsic eruptions. Other than two mafic samples (R01, R02) collected as float near the start of the dive, all samples collected were felsic and quite pumiceous, with 20–25 vol% vesicles. The felsic samples contain phenocrysts of quartz and/or pyroxene near the base of the section and become aphyric upsection. R02 and R04–06 contain 5–10 vol% quartz phenocrysts, R05, R06, and R08 contain 5 vol% pyroxene phenocrysts.

The sequence of felsic pyroclastics observed during HPD1013 probably was deposited as a result of chaotic outflow from the caldera due to voluminous felsic eruptions, perhaps leading to caldera formation. These pyroclastic deposits are

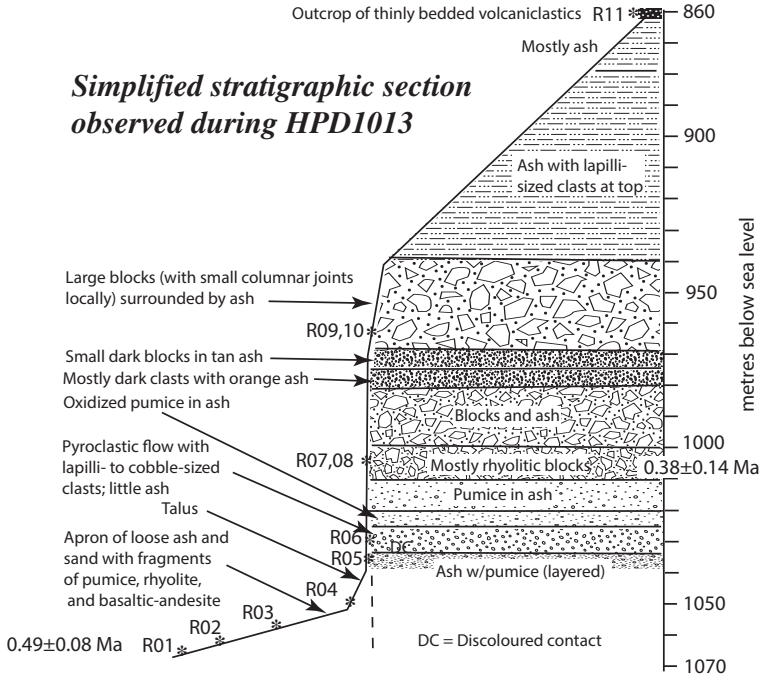

Fig. 6. Simplified stratigraphic column of felsic pyroclastic beds observed on breached southern wall of East Diamante volcano, as traversed during HPD1013. Profile shows approximate slopes, location of rock samplings, (R01–R11), lithostratigraphy and relative thickness of beds.

similar to the youngest units exposed at West Rota volcano (Stern *et al.* 2008). It is unlikely that these erupted from existing dacitic domes, because coarse pyroclastics should have buried these domes if the eruption produced 100 m thick deposits at the site of HPD1013. These are probably resurgent domes, emplaced after caldera formation.

Even more striking evidence of violent felsic eruptions that may be linked to formation of the East Diamante caldera formation is seen north of the northern breached caldera wall, where a well-preserved field of giant sediment waves extends at least 20 km north and is as wide as 30 km. These sediment waves have unusually long wavelengths (1–2 km) and amplitudes (*c.* 100 m tall). The waves are crudely concentric around the northern part of East Diamante and the field broadens with distance from the volcano, indicating that these probably resulted from unusually strong currents emanating from the region now occupied by the caldera. The impression that these sediment waves may be a far-field manifestation of a violent submarine eruption ('Neptunian'; Allen & McPhie 2009) – perhaps some kind of a submarine pyroclastic flow – is strengthened by the observation that such waves are missing on the seafloor NE of the volcano, which was shielded by the high-standing carbonate ridge on the caldera's eastern margin. The presence of the waves immediately downslope from where the northern flank of the caldera is missing is striking circumstantial evidence that the field of giant sediment waves is linked to one or more violent eruptions that accompanied caldera formation. A similar interpretation of the giant sediment waves on the flanks of major arc volcanoes was made by Draut & Clift (2006), although they emphasize bottom currents whereas we emphasize Neptunian eruptions (Allen & McPhie 2009). During one of these eruptions, a 100 m-thick pyroclastic flow (studied during HPD1013) was directed south from the caldera. During or after the last caldera-forming event, rhyodacitic domes were intruded into the caldera and minor dacitic lava flows issued from them. These felsic magmatic systems provided sufficient heat to allow the development of a vigorous hydrothermal system, which is still active.

$^{40}Ar/^{39}Ar$ geochronology

Because they are built on Mariana Trough crust, the Diamante volcanoes must have grown after the back-arc basin opened beginning *c.* 5 Ma (Stern *et al.* 2003). Table 1 and Figure 7 summarize three

Table 1. *Results of stepwise-heating analyses of volcanic rocks from the studied area*

Analysis no.	Station & sample no.	Total age ($\pm 1\sigma$)				Plateau age ($\pm 1\sigma$)				
		Integrated age (Ma)	Inverse isochron age (Ma)	$^{40}Ar/^{36}Ar$ intercept	MSWD	Weighted average (Ma)	Inverse isochron age (Ma)	$^{40}Ar/^{36}Ar$ intercept	MSWD	Fraction of ^{39}Ar (%)
U11037	HPD1012R7	0.040 ± 0.008	0.021 ± 0.004	301.1 ± 2.1	0.86	0.020 ± 0.004	0.013 ± 0.009	312 ± 23	0.36	71.4
U11302	HPD1013R1	0.47 ± 0.09	0.61 ± 0.15	291 ± 7	1.32	0.47 ± 0.08	0.61 ± 0.15	291 ± 7	1.32	100.0
U11357	HPD1013R8	0.36 ± 0.16	0.37 ± 0.12	283 ± 39	0.60	0.37 ± 0.14	0.37 ± 0.12	283 ± 39	0.60	100.0

MSWD, mean square of weighted deviates ($\sqrt{SUMS/(n-2)}$) in York (1969).
Integrated ages were calculated using sum of the total gas released.
$l_b = 4.962 \times 10^{-10}\ a^{-1}$, $l_e = 0.581 \times 10^{-10}\ a^{-1}$, $^{40}K/K = 0.01167\%$ (Steiger & Jäger 1977).

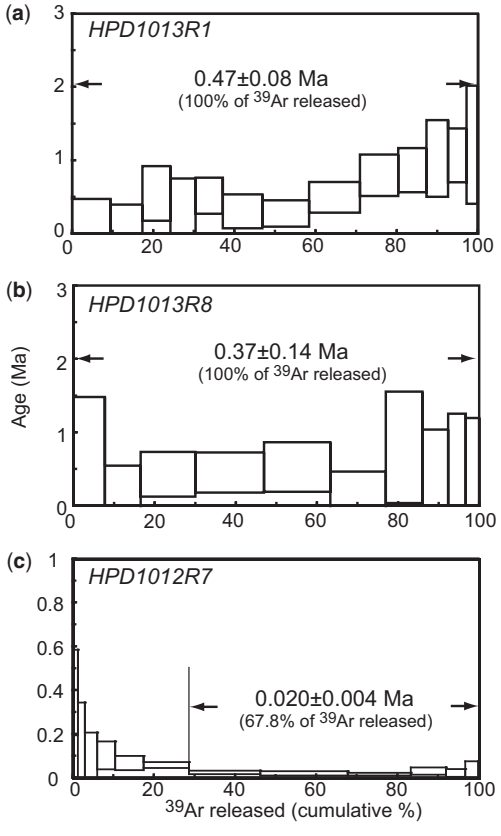

Fig. 7. $^{40}Ar/^{39}Ar$ age spectrum for (**a**) East Diamante basaltic andesite sample HPD1013 R01; (**b**) East Diamante felsic pyroclast sample HPD1013 R08; (**c**) Dacite sample HPD1012-R07 from a felsic dome in East Diamante caldera.

new $^{40}Ar/^{39}Ar$ whole-rock ages for East Diamante samples (techniques and results can be found in the Supplementary material). The oldest one is for a basaltic andesite recovered as float from the base of the section sampled during HPD1013 (R01; Fig. 6), which yields a plateau age of 0.47 ± 0.08 Ma (Fig. 7a). A felsic sample (HPD1013R8) from *c.* 70 m higher (Fig. 6) is from the first coarse pyroclastic layer in this section. This yields a plateau age of 0.37 ± 0.14 Ma (Fig. 7b). Finally, we have one $^{40}Ar/^{39}Ar$ age for a felsic whole-rock sample (HPD1012 R7; Fig. 5) from a dacite (68.6 wt% SiO_2; 1.6 wt% K_2O) collected from a small knoll inside East Diamante caldera. This yields an age of 20 000 ± 4000 years (Fig. 7a; Supplementary material).

We interpret these three ages to indicate the following sequence of events. Construction of a stratovolcano began before *c.* 0.5 Ma and culminated in violent felsic volcanism beginning *c.* 0.38 Ma. The present East Diamante caldera began to form about this time or later. Felsic igneous activity including emplacement of resurgent dacite domes followed caldera formation, continuing up to *c.* 20 ka. Such a youthful age is consistent with other evidence that East Diamante is a dormant volcano, including continued vigorous hydrothermal activity associated with felsic domes inside the caldera.

Diamante cross-chain petrology and chemical composition

Basalts were recovered from all three volcanoes. Basalts from East Diamante are porphyritic, with phenocrysts of 20–30 vol% plagioclase, 0.2–0.7 vol% olivine, and 0.5–5 vol% clinopyroxene (Fig. 8d). More differentiated basalts contain orthopyroxene and magnetite instead of olivine. Basalts from Central Diamante and West Diamante contain more olivine (1–4 vol%) and less plagioclase (10–20 vol%) than do East Diamante basalts. Clinopyroxene is rare in Central Diamante lavas, but 7–10 vol% clinopyroxene is typical in West Diamante basalts. East Diamante andesites contain 4–6 vol% plagioclase and <1 vol% clinopyroxene ± orthopyroxene (Fig. 8a). Dacites and rhyolites are found only from East Diamante and comprise two general types. One is porphyritic, containing plagioclase (17–30 vol%), quartz (4–10 vol%), *c.* 1 vol% clinopyroxene, 1–2 vol% orthopyroxene and 0.2–0.3 vol% magnetite (Fig. 8b, c). The other type is aphyric, with <3 vol% phenocrysts and is two-pyroxene plagioclase dacite.

Eighty-one volcanic rocks from the Diamante cross-chain were analysed for major and limited trace element abundances. Data in the compilation include five analyses from Dixon & Stern (1983), 15 analyses of Cook 7 (D34, D37, D38 D59, and D60) samples, three analyses of samples collected during TT167 ROPOS dive 787 (Fig. 5), and 58 analyses of samples collected during NT09–08 HPD1011–1018 and NT10–12 HPD1150–1154 dives. Only the data of Dixon & Stern (1983) have been previously published; the other 76 analyses are listed in the Supplementary material. These 81 analyses are distributed between the three major volcanic centres: 51 samples from East Diamante (including 4 parasitic cones on its flanks), eight samples from Central Diamante, and 21 samples from West Diamante. For ease of comparison, major element data discussed below have been normalized to 100wt% anhydrous, but sums of the original analyses are also reported in the Supplementary material.

Fig. 8. Representative photomicrographs (crossed-polarized light) of East Diamante igneous rocks, 100 μm-scale bar (black) in lower left applies to all images. P, plagioclase; Qz, quartz; O, orthopyroxene; C, clinopyroxene; Ol, olivine; white V, void. Note that plagioclase phenocrysts in felsic samples (**b**, **c**) show oscillatory zoning whereas those in basalt from NNW parasitic cone sampled by HPD1015 (**d**) show cloudy interiors, evidence of magma mixing.

These lavas range from primitive basalts (*c.* 10 wt% MgO and maximum Mg # (=100 Mg/Mg + Fe) = 68) to rhyolite (maximum SiO_2 = 75.4 wt%). The three volcanoes show different extents of differentiation, with West Diamante erupting the most primitive lavas (mean SiO_2 = 52.2 ± 2.2 wt%; mean Mg# = 55 ± 8.3) through mostly mafic but fractionated Central Diamante (mean SiO_2 = 54.8 ± 7.1 wt%; mean Mg# = 39.9 ± 5.5) to East Diamante (mean SiO_2 = 63.1 ± 9.0 wt%; mean Mg# = 40 ± 10.2). The lavas are strongly bimodal in silica Fig. 9), with mafic lavas containing 50–58 wt% SiO_2 and felsic samples containing 66–76 wt% SiO_2. There is a marked silica gap between 58 and 66 wt% SiO_2, which is best seen in the data for East Diamante (Fig. 9a). This bimodal variation is similar to lavas from Sumisu caldera in the Izu arc (Tamura *et al.* 2005). All 21 West Diamante samples are mafic, with 49–57 wt% SiO_2 (Fig. 9c). All but one of the analysed lavas from Central Diamante are mafic (50–53 wt% SiO_2; Fig. 9b).

Insights into the nature of Diamante cross-chain lavas can be gained from examining plots of FeO*/MgO v. SiO_2 (Fig. 10a) and Na_2O v. MgO (Fig. 10b). The FeO*/MgO v. SiO_2 diagram shows that East Diamante lavas have similar FeO*/MgO of 2–4 in spite of very different SiO_2 contents. Most mafic Diamante lavas plot in or near the tholeiitic field, whereas most felsic lavas plot in the calc-alkalic field. Arculus (2003) has criticized the tholeiitic/calc-alkalic diagram and argued that it makes more petrological sense to distinguish between high-Fe, medium-Fe and low-Fe suites (Fig. 10a). East Diamante mafic lavas mostly plot in the high-Fe field, well within the tholeiitic field whereas East Diamante felsic lavas are all calc-alkalic, plotting near the medium-Fe–low-Fe divide. Arculus (2003, p. 932) emphasized that his 'boundaries have been drawn as far as possible to ensure that various suites currently asserted to be dominantly formed by fractional crystallization remain within a given field'. Because East Diamante mafic and felsic lavas plot in different fields,

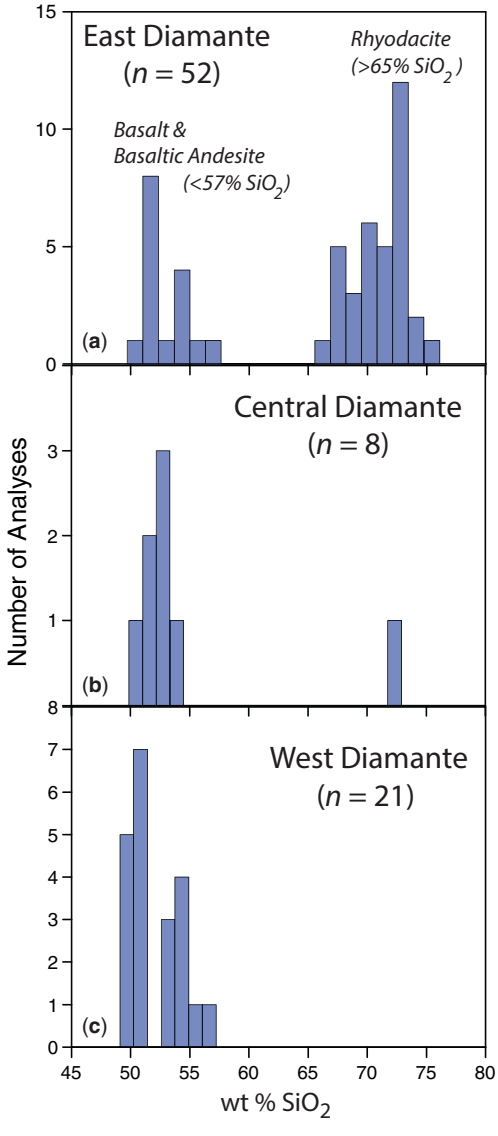

Fig. 9. Silica histograms for Diamante cross-chain lavas (recalculated 100 wt% anhydrous). (**a**) East Diamante volcano; (**b**) Central Diamante volcano; (**c**) West Diamante volcano. *n*, number of analyses.

they appear to be unrelated by simple fractional crystallization. In contrast, Central Diamante lavas cluster tightly around the high-Fe/medium-Fe boundary, with one felsic lava plotting similarly but at higher silica content. West Diamante lavas are mostly low-Fe suites but some also plot in the medium-Fe field.

The Na_2O v. MgO relationships of Diamante cross-chain lavas are shown in Figure 10b. All data define Na_6 (Na_2O content at 6 wt% MgO; Plank & Langmuir 1988) *c.* 2.46 wt%, and moderately correlate ($r^2 = 0.83$). This is similar to the average Na_6 value of 2.4 ± 0.42 wt% that Plank & Langmuir (1988) calculated for three Mariana arc volcanoes (Maug, Pagan and Sarigan). Treating each of the three Diamante cross-chain volcanoes separately yields East Diamante Na_6 ~2.5 wt% ($r^2 = 0.64$), Central Diamante Na_6 ~1.62 wt% ($r^2 = 0.94$) and West Diamante Na_6 ~2.5 wt% ($r^2 = 0.82$). Samples from East Diamante have a range in Na_2O content at the same (3–5 wt%) MgO contents. This may reflect different primary basalt magmas resulting from different degrees of mantle melting as discussed by Tamura *et al.* (2005). Plank & Langmuir (1988) related Na_6 to the height of the melting column (*c.* depth to subduction zone minus crustal thickness); if this were the important control for Diamante cross-chain lavas, Na_6 should be highest (shortest melting column) beneath East Diamante and lowest (longest melting column beneath West Diamante. Clearly there are other important controls on the extent of melting manifested by Na_2O–MgO relationships for Diamante cross-chain lavas.

The only primitive lavas (i.e. those with Mg# >65, generally >8 wt% MgO) are from Cook7 D60 from West Diamante, although HPD1015 parasitic on East Diamante has Mg# = 62 and erupts lavas with >8 wt% MgO. Fe_6 (FeO* content at 6 wt% MgO) relationships for Diamante cross-chain lavas suggest cross-arc variations in the depth of mantle melting. Fe_6 varies from *c.* 13 wt% beneath Central Diamante to *c.* 8.5 wt% beneath West Diamante (Fig. 11). The correlation coefficient for West Diamante lavas is low but a small variation in FeO* over the interval of 3–10 wt% MgO allows Fe_6 to be estimated with confidence at 8.5 ± 1 wt%. East Diamante lavas show two trends: one suite comprising older lavas from the NE caldera wall whereas samples from the parasitic cone on its WNW flank show lower Fe_6. Other East Diamante mafic lavas define a high-Fe suite, with Fe_6 ~15 wt%. These estimates of Fe_6 encompass the average of 10.6 ± 1.65 wt% for three Mariana arc volcanoes (Maug, Pagan and Sarigan; Plank & Langmuir 1988). Higher Fe_6 beneath the volcanic front is interpreted as deeper mean melting depth due to destabilization of olivine (Kelley *et al.* 2010).

Major element abundances for Diamante cross-chain lavas are plotted against silica in Figure 12. Concentrations of TiO_2, MgO, FeO* and CaO decrease with increasing silica, but the large silica gap breaks the continuity of these trends. The behaviour of TiO_2 (Fig. 12a) and FeO* (Fig. 12d) suggests that a phase rich in these elements, probably magnetite, is residual or crystallized early

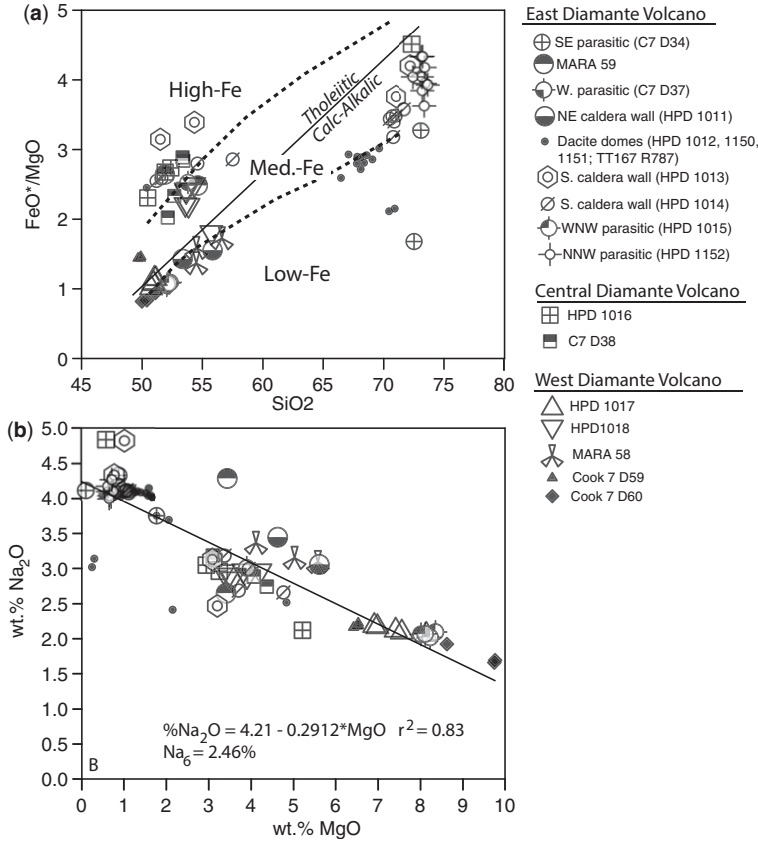

Fig. 10. Geochemical variations observed in Diamante cross-chain igneous rocks. (**a**) wt% FeO*/MgO v. wt% SiO_2 plot of Diamante volcanic rocks. Straight diagonal line separates tholeiitic and calc-alkalic fields of Miyashiro (1974), curved dashed lines separate high-Fe, medium-Fe, and low-Fe fields of Arculus (2003). (**b**) Plot of Diamante volcanic rock wt% Na_2O v. wt% MgO.

during Diamante magmatic evolution. Most Diamante mafic lavas are high-Al basalt, although the Cook 7 D59 and HPD1015 primitive lavas are not (Fig. 12b). The decrease in Al_2O_3 with increasing silica indicates an important role for plagioclase as a fractionating or residual phase. Rapid decrease of MgO with increasing silica (Fig. 12c) indicates an important role for fractionating and/or residual olivine and pyroxene. Monotonically decreasing CaO with silica (Fig. 12e) further indicates control by clinopyroxene and/or calcic plagioclase. Na_2O increases rapidly with increasing silica in mafic rocks, indicating that it is a strongly incompatible element over this silica range; however, as shown in Figure 9b, East Diamante magmas had varying contents of Na_2O, reflecting that of their primary magmas. The K_2O–SiO_2 diagram (Fig. 12g) shows that Diamante cross-chain lavas mostly plot in the medium-K field, although some felsic samples fall in the low-K field. These are typical Mariana arc lavas for the most part, which are characteristically a medium-K suite (Stern *et al.* 2003).

Figure 12 also shows fields for hydrous melting experiments on IBM basalts, intended to capture the composition of liquids generated by melting of mafic IBM arc crust. The dashed fields show the results of Nakajima & Arima (1998), over a P range of 1–1.5 GPa and 2–5 wt% H_2O, whereas the star shows the 'inferred felsic melt' of Tatsumi & Suzuki (2009), determined at 0.3 GPa in the presence of 0.49–2.8 wt% H_2O. These experimental results are similar to the composition of East Diamante felsic lavas except that Na_2O and K_2O of the experimental starting materials are lower. This may be accounted for by the fact that the basaltic starting materials (from the Izu arc) used in these experiments contain less Na_2O and K_2O than do Mariana arc lavas (Stern *et al.* 2003).

Figure 13 summarizes the phenocryst compositions in Diamante cross-chain mafic lavas as

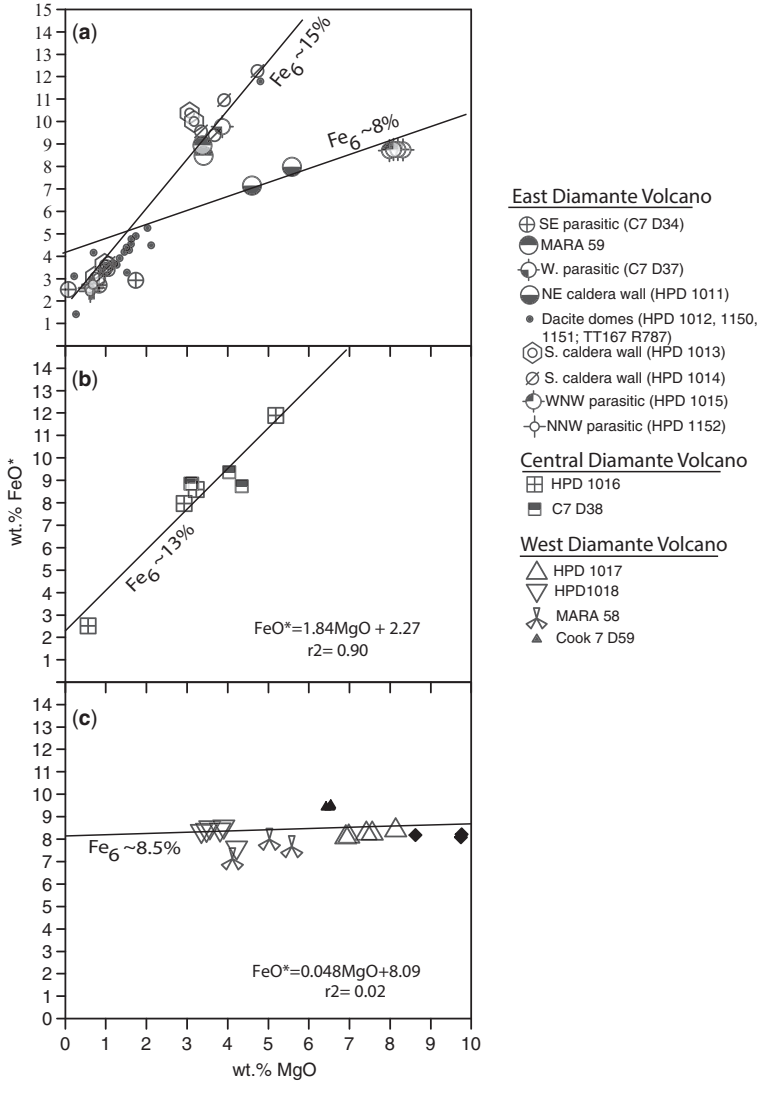

Fig. 11. Plots of wt% FeO* v. wt% MgO for whole-rock samples from (**a**) East Diamante (except HPD1015 samples from parasitic cone and HPD1011older edifice samples); (**b**) Central Diamante; and (**c**) West Diamante.

determined from electron microprobe analyses (Supplementary material). Samples show modest variations in Fo content of olivine and An content of plagioclase except for 1015R01 (from a satellite cone on the WNW flank of East Diamante). This basalt has a primitive major element composition (*c.* 8 wt% MgO) but shows a very wide range of olivine, clinopyroxene and plagioclase compositions (Fig. 13g–i), suggesting mixing of primitive and fractionated magmas. Further evidence of mixing is manifested by the presence of many resorbed plagioclase phenocrysts in these lavas. Central Diamante samples show slightly more magnesian olivines (~Fo75) in equilibrium with slightly less calcic plagioclase (~An85), but the range of plagioclase compositions (Fig. 13l, o) suggests magma mixing. Lavas from West Diamante volcano show a range of olivine compositions (~Fo78–90) in association with calcic plagioclase compositions (~An80–90). From these results, there is evidence of mixing of mafic and very evolved magmas beneath Central Diamante and the western flank of East Diamante volcano.

Electron microprobe results for coexisting olivine and plagioclase in the Diamante cross-chain mafic lavas are summarized in Figure 14.

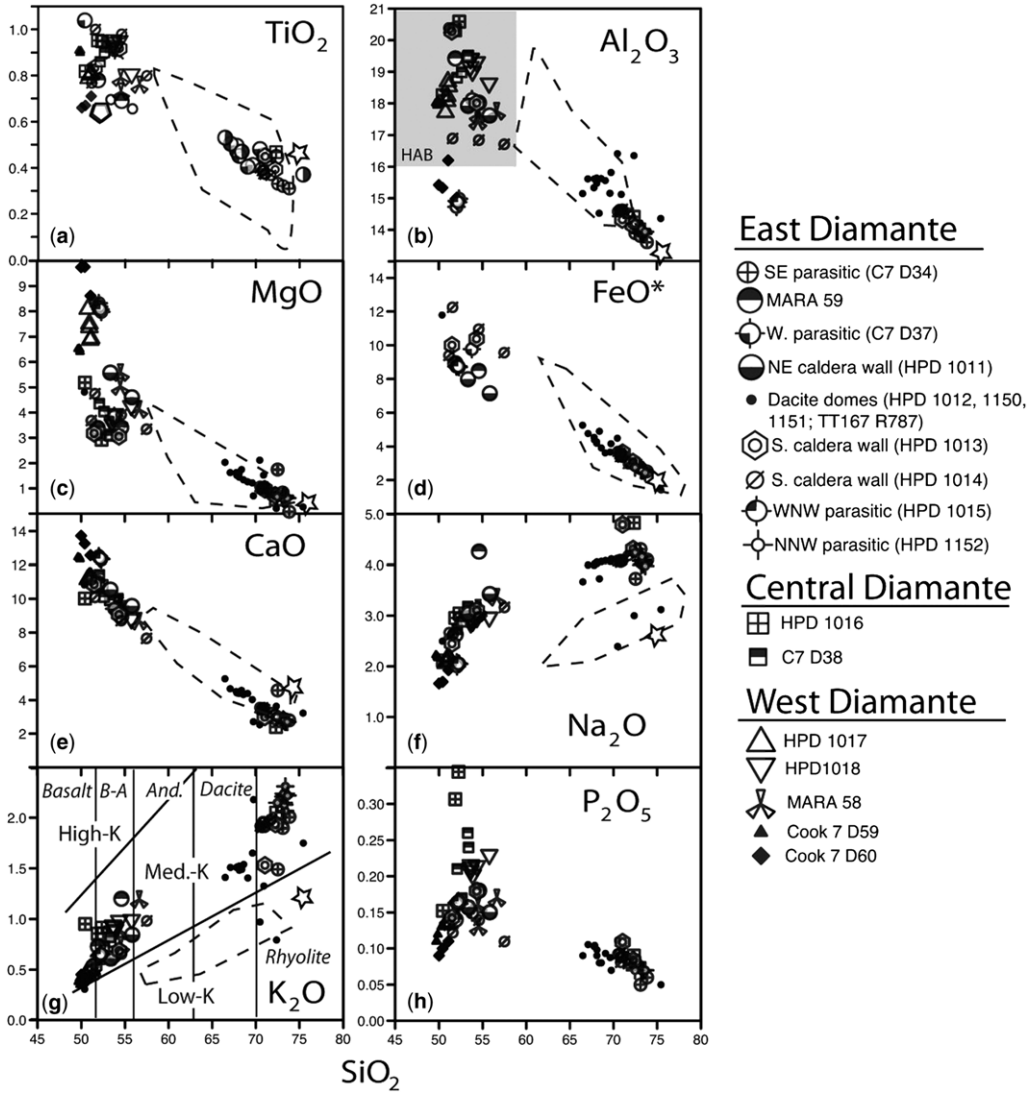

Fig. 12. Harker variation diagrams for Diamante cross-chain volcanic rocks (all oxides in wt%). (**a**) TiO_2 v. SiO_2. (**b**) Al_2O_3 v. SiO_2. Grey field labelled 'HAB' shows field of high-alumina basalt (Crawford *et al.* 1987). (**c**) MgO v. SiO_2. (**d**) Total iron as FeO v. SiO_2. (**e**) CaO v. SiO_2. (**f**) Na_2O v. SiO_2. (**g**) K_2O v. SiO_2. East Diamante lavas mostly plot within the medium-K (calc-alkaline) field, although some samples plot in the low-K field. (**h**) P_2O_5 v. SiO_2. Dashed fields in (a)–(g) encompass experimental melts of tholeiitic metabasalt, 1–1.5 GPa, 2–5 wt% H_2O (Nakajima & Arima 1998). Star in (a)–(g) indicates composition of 'inferred felsic melt' generated by hydrous melting of Izu arc tholeiite at 0.3 GPa (*c.* 10 km depth; Tatsumi & Suzuki 2009).

Most Diamante cross-chain basalts contain coexisting Fe-rich olivine (~Fo70) and Ca-rich plagioclase (~An90), characteristic of arc basalts (Stern 2010). Even the volcanoes behind the volcanic front – Central and West Diamante volcanoes – show Fo–An relations that are arc-like, in contrast to the situation for the Guguan cross-chain to the north. Interestingly, only HPD1015 primitive 'mixed' basalt plots in the field defined by OIB and MORB.

Figure 15 summarizes equilibrium temperatures for four East Diamante igneous rocks that contain two pyroxenes, which permit magmatic temperatures to be estimated using the two-pyroxene thermometer of Lindsley & Andersen (1983). These samples are fractionated, with one basaltic andesite

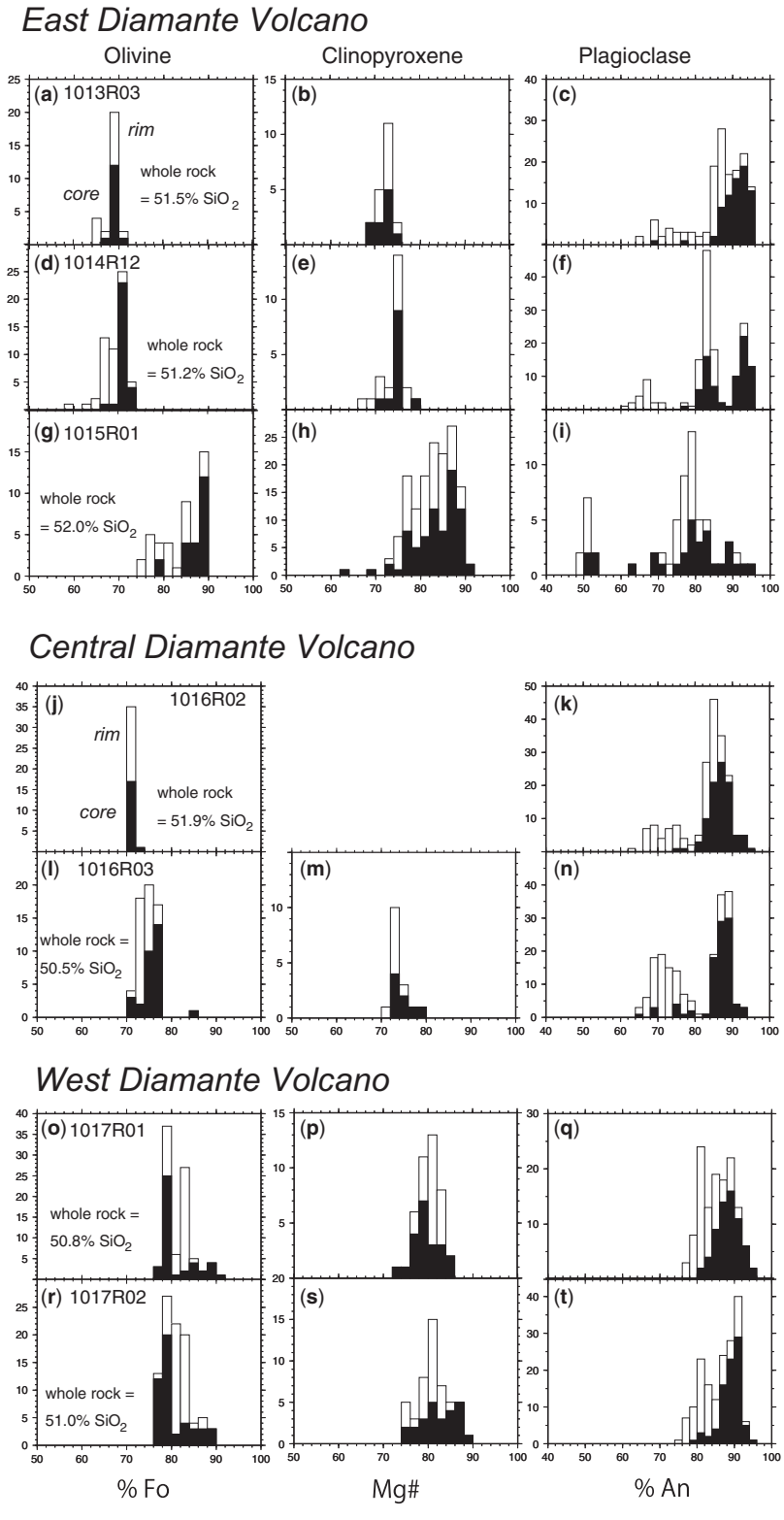

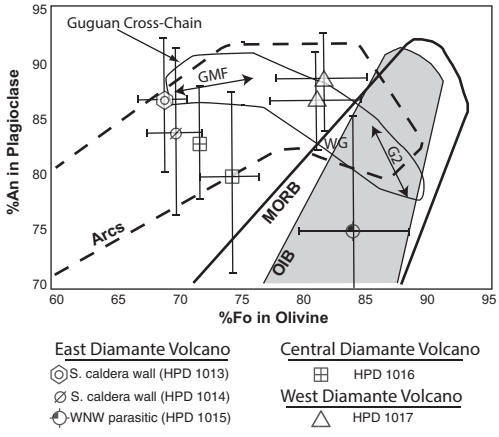

Fig. 14. Plagioclase mol% An content v. olivine mol% Fo for lavas from Diamante cross-chain volcanoes ($\pm 1\sigma$), modified after Stern *et al.* (2006). Note strong cross-arc variation for Guguan samples, from low Fo/high An for samples from Guguan volcanic front lavas (GMF) to OIB- and MORB-like assemblages (high Fo/low An compositions) for Guguan 2 (G2), farthest from the trench; W Guguan (WG) which lies between the two volcanoes has intermediate compositions. Such strong cross-arc variations in Fo–An compositional relations are not seen for Diamante cross-chain samples which (except HPD1015) plot in the arc field.

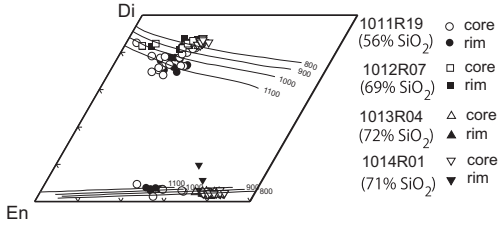

Fig. 15. Coexisting pyroxene compositions for East Diamante lavas, one basaltic andesite and three rhyodacites, plot is left side of pyroxene quadrilateral; Di, diopside; En, entatite. Tick marks are at 10 mol%. Whole-rock SiO_2 abundances (in wt%) are given in parentheses for each sample. Magmatic equilibration temperatures for both cores and rims are estimated using the two-pyroxene thermometer of Lindsley & Andersen (1983). Both core and rim compositions of individual phenocrysts are plotted in each sample.

and three dacites. This is a graphical thermometer; temperature of pyroxenes can be inferred from plotting compositions on a Ca–Mg–Fe diagram (Fig. 15). Both core and rim compositions of individual phenocrysts are plotted for each sample (compositional data can be found in the Supplementary material). Basaltic andesite sample HPD1011-R19 gives higher temperatures of *c.* 1000–1100 °C, whereas temperatures calculated for the three felsic rocks indicate relatively low temperatures of *c.* 800 °C. Augite in sample 1012-R07 scatter because some may have been derived from mafic inclusions, but many others plot close to T ~ 800 °C.

Data for a limited number of trace elements are summarized in Figure 16. Figure 16a shows Rb variations, which scatter to somewhat higher concentrations with silica. Ba increases more consistently with silica (Fig. 16b). Sr decreases with SiO_2, indicating that plagioclase exerts an important control. Zr also scatters to higher values with silica (Fig. 16d). Y defines two groups for the felsic samples, a low-Y (15–30 ppm) group defined by East Diamante samples from most of the resurgent domes, HPD1014 samples from the southern caldera wall, and the NNW parasitic cone, and a high-Y group defined by the SE parasitic cone, HPD samples from the southern caldera wall, and the felsic sample from Central Diamante volcano (Fig. 16e). Rb/Ba decreases with increasing silica (Fig. 16f), which is difficult to explain by crystal fractionation because both elements are highly incompatible. Sr/Y decreases strongly with silica (Fig. 16g), further indicating that Diamante magmas evolved by low-P (garnet-free) fractionation or anatexis. Zr/Y is generally lower in mafic samples than felsic samples (Fig. 16h). Among the felsic samples, samples from the resurgent domes, HPD 1014 samples from the S. caldera wall, and the NNW parasitic cones have higher Zr/Y than samples from the SE parasitic edifice and HPD 1013 samples from the southern caldera wall.

Discussion

Felsic volcanism in intra-oceanic arcs is increasingly recognized, but how and why these magmas form is controversial. The Diamante cross-chain provides some useful constraints for answering this question. One important feature of this felsic magmatic system seems to be that it has persisted for a significant length of time; in the case of East Diamante, a magmatic history encompassing at

Fig. 13. Summary of electron microprobe results for phenocrysts in seven Diamante cross-chain lavas: mol% Fo in olivine (left column), atomic Mg# in clinopyroxene (centre column) and mol% An in plagioclase (right column). Vertical axes are numbers of analyses. Whole-rock silica contents are also given in left panels (in wt%). Core and rim compositions are given as dark and light bars.

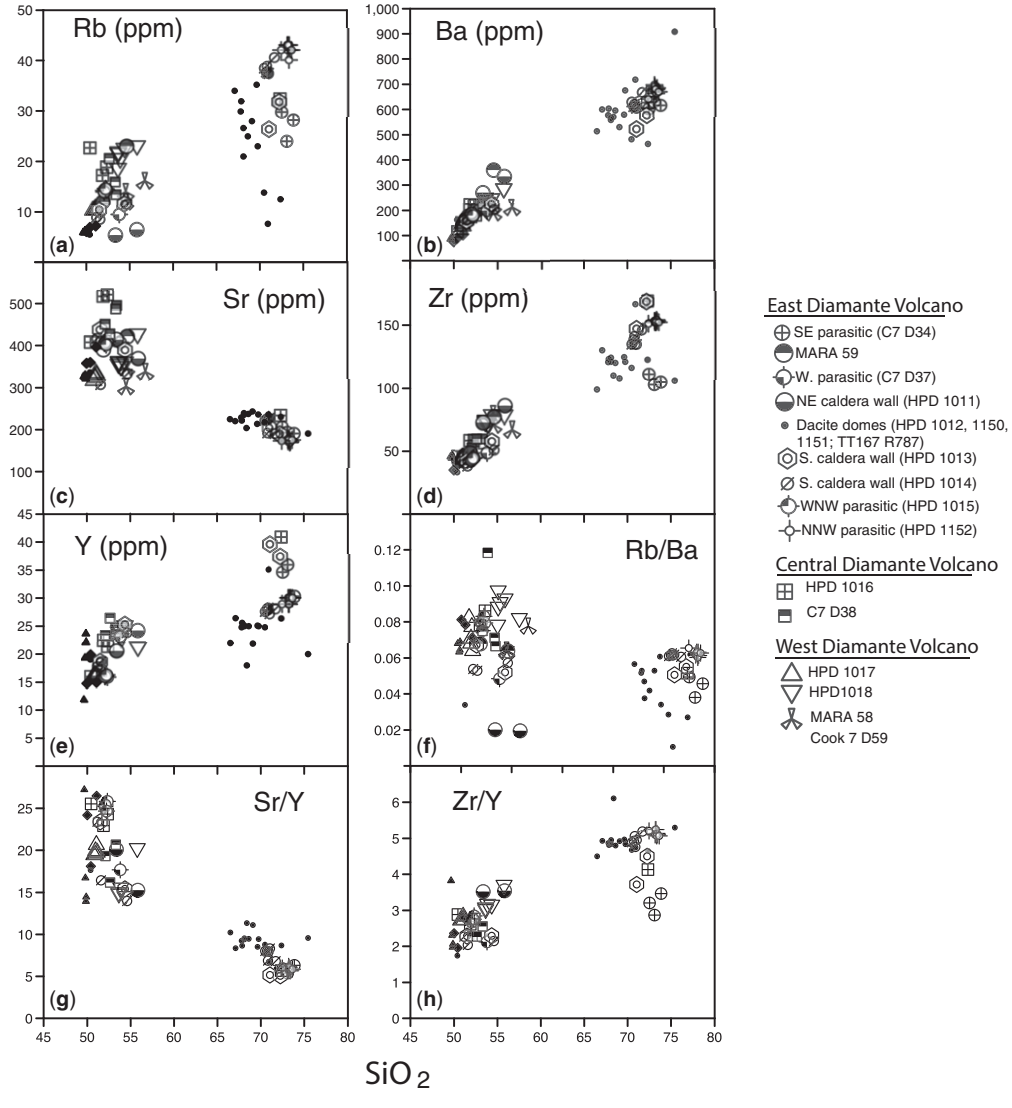

Fig. 16. Selected trace element concentrations (in ppm) and ratios in Diamante volcanic rocks as a function of wt% SiO_2: (**a**) Rb v. SiO_2; (**b**) Ba v. SiO_2; (**c**) Sr v. SiO_2; (**d**) Zr v. SiO_2; (**e**) Y v. SiO_2; (**f**) Rb/Ba v. SiO_2; (**g**) Sr/Y v. SiO_2; (**h**) Zr v. SiO_2. See text for further discussion.

least 0.5 Ma is indicated, although the volcano was dormant long enough to allow a thick carbonate bank to form on its flanks. Violent eruption of volatile-rich felsic magmas beginning at *c.* 0.38 Ma shaped the modern caldera and affected the surrounding seafloor. We suspect that the giant dune fields on the north flank of East Diamante formed during one or more of these events. Quieter emplacement of degassed felsic magma followed, including emplacement of resurgent dacite domes followed caldera formation, continuing up to *c.* 20 ka. But age of the volcano cannot be the only important control on whether or not felsic magmas are present, there are other Mariana volcanoes, such as Pagan and Asuncion, which are larger and thus are likely to be of similar age but which do not erupt felsic lavas.

We do not definitively resolve how East Diamante felsic magmas formed here because we have limited trace element and no isotopic data; those results and analysis will be presented elsewhere. There are several pertinent observations from our data that are noteworthy. First, these are not slab melts (adakites), because Sr/Y of felsic

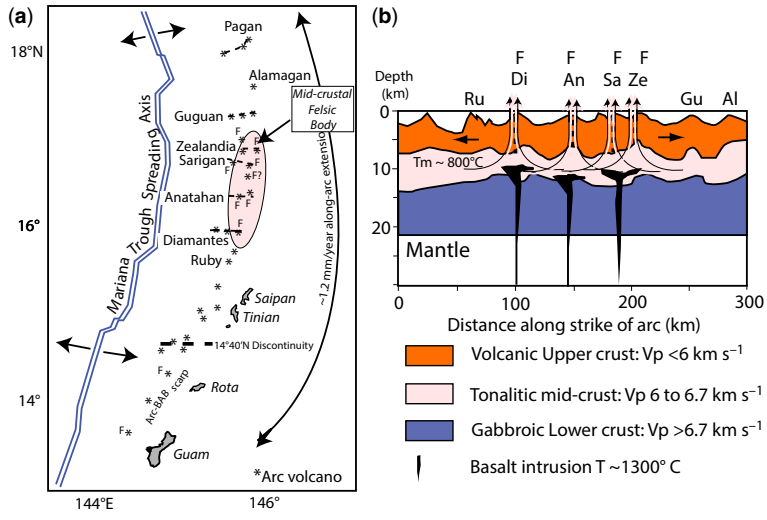

Fig. 17. Anatahan Felsic Province location and how these melts might be generated. (**a**) Simplified map showing the distribution of arc volcanoes (*) and back-arc basin spreading axis (double solid line 'Mariana Trough Spreading Axis'). Location of volcanoes with significant felsic volcanism 'F' in the south-central Mariana arc, defining the Anatahan Felsic Province. Along-arc extension rate of 1.2 mm a^{-1} occurs between Guam and Agrigan (not shown, just north of Pagan; Kato *et al.* 2003). The distribution of felsic igneous rocks in the AFP suggests that this region is underlain by a felsic body in the middle crust that is able to escape to the surface because of cross-arc extensional faults (dashed lines) at the Diamantes, Anatahan, Sarigan and Zealandia. Cross-arc extensional zones associated with the Guguan cross-chain to the north and 14°40′N discontinuity to the south do not involve mid-crustal felsic magmas. (**b**) Cross-section (based on Calvert *et al.* 2008, fig. 12a). Mantle-derived mafic magmas *c.* 1300 °C intrude and pond near or within felsic middle crust, which melts *c.* 800 °C. Mafic injection remobilizes felsic middle crust, which escapes to the surface as a result of along-arc extension.

lavas is low (<10; Fig. 16g). Adakites have >56 wt% SiO_2 and Sr/Y >30 (e.g. Castillo 2006). The low Sr/Y characteristic of East Diamante felsics indicates these are part of an 'andesite–dacite–rhyolite' (ADR) suite formed by low-P processes dominated by feldspar, including magmatic fractionation and crustal anatexis.

East Diamante felsic lavas are good examples of cool, wet, oxidized felsic melts. Felsic magmas can be generated either by fractionation of dry mafic magmas generated by decompression mantle melting to yield hot felsic melts, or above subduction zones dominated by flux melting of the mantle, producing cooler, more oxidized and wetter felsic magmas (Bachmann & Bergantz 2009). Christiansen (2005) identified two different types of large volume (>1000 km^3) felsic eruptions of Cenozoic age in the western USA. 'Yellowstone-type' ignimbrites are sparsely phyric and characterized by anhydrous mineral assemblages. These magmas formed by fractional crystallization of more mafic precursors under low oxygen fugacity conditions. Such lavas show crystallization temperatures of 830 to 1050 °C and are characteristic of hotspot magmatic provinces, such as the Snake River Plain. In contrast, 'Fish Canyon-type' ignimbrites are phenocryst-rich and evolved under high water and oxygen fugacity conditions characteristic of continental magmatic arcs. These felsic magmas have pre-eruption temperatures of 730–820 °C and probably formed by crustal melting. Bachmann & Bergantz (2009) summarized evidence that eruption of these magmas reflect interstitial melt trapped within large, upper crustal mush zones, and that interstitial melt extraction is most efficient when mush zones contain 50–60 vol% crystals that produce a semi-rigid framework that hinder chamber-wide convection currents but the permeability is still high enough that interstitial melt can flow between the crystals.

Diamante magmas clearly formed in the crust, at pressures where plagioclase controlled magmatic evolution, via magmatic differentiation or by partial melting of juvenile arc crust. We do not have a full spectrum of geochemical and isotopic data needed to show how these melts formed but several lines of evidence indicates formation mostly by crustal melting, not fractionation. First, East Diamante felsic igneous rocks are part of a bimodal population, with a marked silica gap between 58 and 66 wt% SiO_2. Similar to the conclusions reached by Shukuno *et al.* (2006) for the bimodal igneous

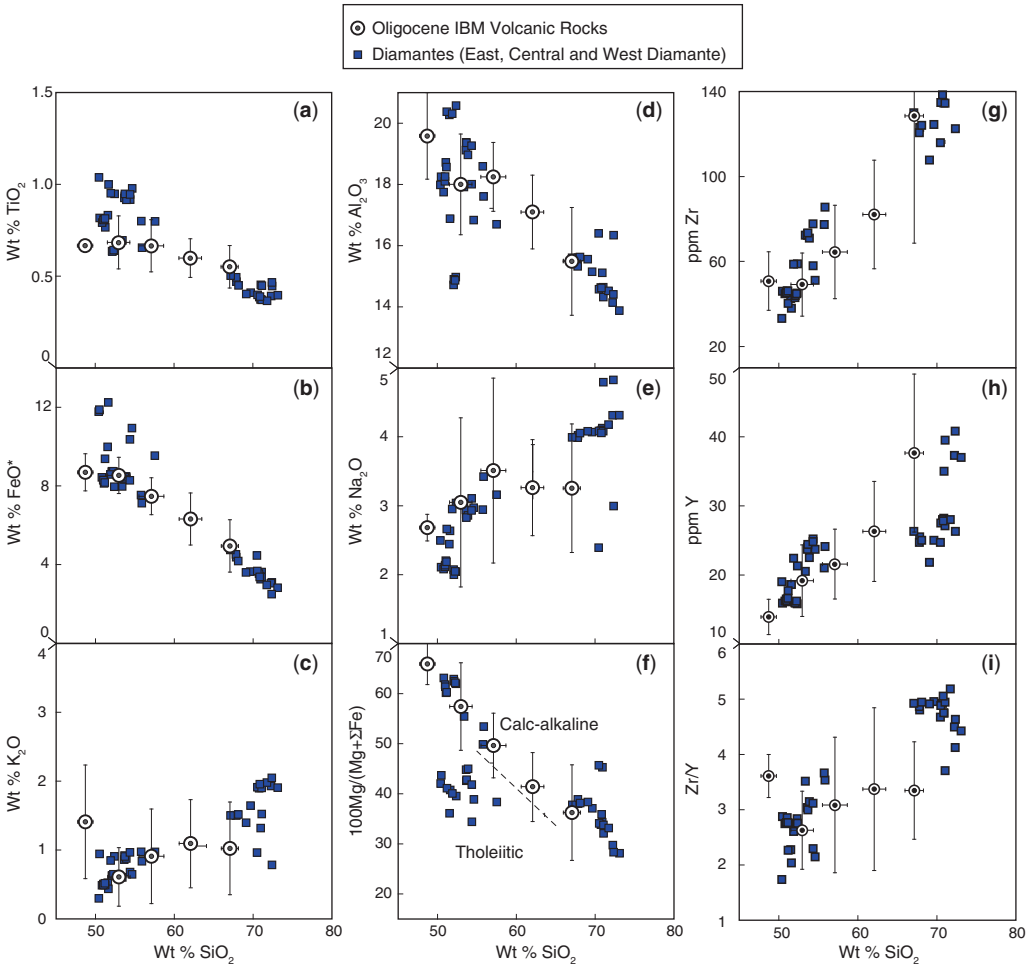

Fig. 18. Comparison of lava compositions from Diamante cross-chain volcanoes with IBM Oligocene rocks and collision zone plutons (Tamura *et al.* 2010). Diamante lavas are compositionally similar to Oligocene volcanic rocks of the Izu arc. Tamura *et al.* (2010) proposed that IBM arc middle crust involved in the collision with Honshu was partially melted during the collision and then intruded into the overlying upper crust of the Honshu and IBM arcs. The similarity of Oligocene middle crust to Diamante and other felsic AFP lavas suggests that remobilization of this crust may also occur under extension.

rocks of Sumisu volcano in the Izu arc, it is difficult to understand how fractionation of mafic parental magma would cause such a silica gap. It is correspondingly easier to understand how felsic melts formed as part of a bimodal suite by crustal melting at 800 °C as a result of heating by emplacement of *c.* 1200 °C mafic magmas into the crust.

The widespread occurrence of felsic lavas in the region including and north of the Diamante seamounts indicates that felsic magmas do not form in magma chambers associated with individual volcanoes and that instead there is a regional source for these magmas. East Diamante is the southernmost of at least seven volcanoes that have recently erupted significant volumes of felsic magmas. This region encompasses *c.* 110 km along the Mariana arc and was identified as the Anatahan Felsic Province (AFP) by Stern & Hargrove (2003; Fig. 17). East Diamante is the southernmost representative of AFP volcanism. To the north in the AFP, Anatahan erupted dacites with up to 66 wt% SiO_2, most recently in 2003 (Wade *et al.* 2005). Dacite with up to 66 wt% SiO_2 was also recovered during Cook 7 from a submarine volcano *c.* 15 km NE of Anatahan. Sarigan erupted lavas with up to 61 wt% SiO_2 (Woodhead 1989). Dacite with up to 66 wt% SiO_2 was recovered during Cook 7 from a submarine volcano west of Sarigan. NT0908

explored Zealandia crater and recovered dacites with up to 72 wt% SiO_2. Dacite with up to 61 to 66 wt% SiO_2 was also recovered from a seamount west of Zealandia Bank during Cook 7. In addition to these seven AFP sites where felsic lavas are known, a seamount south of Sarigan seems to have exploded felsic pyroclastic material from 300 m below sea level up to 12 000 m in the atmosphere in May 2010 (Green *et al.* 2013). Such an explosive eruption was likely to have been a felsic eruption, but there are no analyses of this material to confirm or refute this suggestion.

Volcano size – proxy for age and, hence, evolved magmatic storage systems – does not control the distribution of felsic lavas in the AFP. This is also seen for small felsic plugs or cones on the flanks of East Diamante, including those sampled by Cook 7 D34 and HPD1152. We suggest that AFP felsic magmas are derived from the 3–5 km thick 'tonalite layer' imaged in the mid-crust, with V_p = 6.1–6.5 km s^{-1}, beneath volcanic front edifices (Fig. 3; Takahashi *et al.* 2007). Crustal structure beneath Mariana volcanic front edifices has also been studied by Calvert *et al.* (2008). These studies show that the middle crust is thickest beneath the volcanic front. Bimodal volcanism at the volcanic front (East Diamante) suggests that interaction of hot (*c.* 1200 °C), wet (3 wt% H_2O), mafic magmas with tonalitic middle crust helps generate East Diamante felsic magmas. Evidence of this interaction may be present in the disequilibrium textures in basaltic lavas sampled during HPD1015. The mid-crustal tonalitic layer tapers away to the west, where basaltic rear-arc cross-chain volcanoes are found, and this may be why felsic lavas are rare in Central Diamante and unknown in West Diamante.

Structural controls may also be important for AFP volcanism. Christiansen (2005) argued that viscous low-T felsic magmas could erupt only when the roof over the magma body collapsed. Thus eruption and emplacement of AFP felsic magmas may also have been favored by strong along-arc extension affecting the Marianas. GPS measurements indicate that extension between Agrigan and Guam is occurring at nearly 12 mm a^{-1} (Kato *et al.* 2003). There is insufficient spatial resolution in the GPS data to reveal whether extension is uniform or localized, but several lines of evidence indicate that this strain is localized in discrete zones. These include east–west orientations of individual volcanoes, such as East Diamante and Anatahan, alignments of volcanic chains, such as Guguan and Diamante cross-chains, and crustal earthquake swarms near 14°30′N, beneath Central Diamante, and west of Sarigan (Heeszel *et al.* 2008). These approximately east–west-oriented zones of extension allow felsic magmas, if present, to erupt. This is the case beneath East Diamante but the felsic magma body does not seem to extend far enough west to be tapped by West Diamante volcano.

The idea that AFP felsic volcanism is the result of re-melting Mariana middle crust is supported when the composition of Diamante cross-chain lavas are compared with the similar composition of Oligocene igneous rocks studied by Tamura *et al.* (2010; Fig. 18). They proposed that IBM arc middle crust involved in the collision with Honshu was partially melted during the collision and then intruded into the overlying upper crust of the Honshu and IBM arcs. The similarity of Oligocene middle crust to Diamante and other felsic AFP lavas suggests that remobilization of this crust may also occur under extension.

The regional distribution of felsic volcanism in the AFP and its association with along-arc extension are the most convincing observations to us that this felsic volcanism is due to re-melting of tonalitic middle arc crust, not due to fractionation of mafic melts. Future studies to test these ideas are in progress.

Conclusions

Lavas erupted from three submarine volcanoes of the Diamante volcanic cross-chain in the Mariana arc provide useful perspectives on intra-oceanic arc felsic magmagenesis and eruption. New data from five dredges and 13 ROV dives during four research expeditions indicate that cross-chain magmas formed by interaction of subduction-related basaltic flux from the mantle focused along an east–west extension zone that traversed thick arc crust in the east and refractory back-arc basin crust in the west. East Diamante volcano is by far the largest of the three volcanoes and has a well-developed (5 × 10 km), structurally controlled (elongate east–west) caldera. East Diamante mafic volcanism began at least as early as 0.47 ± 0.08 Ma ($^{40}Ar/^{39}Ar$ age) and the volcano had quiescent intervals that were long enough to construct a *c.* 400 m thick sequence of Plio-Pleistocene carbonate sediments. Timing of caldera formation is approximated by $^{40}Ar/^{39}Ar$ age of 0.37 ± 0.14 Ma for a felsic tuff fragment in a thick pyroclastic sequence. Caldera formation was followed by emplacement of resurgent dacite domes, one of which is young enough ($^{40}Ar/^{39}Ar$ age of 20 000 ± 4000 years) to provide sufficient heat to power a vigorous hydrothermal system. In contrast to the large and complex East Diamante volcano, West Diamante is a simple basaltic edifice, whereas the smallest edifice, Central Diamante has erupted minor felsic magmas and is affected by east–west normal faulting.

Eighty-one analyses of rock major element and selected trace element compositions reveal that Diamante cross-chain lavas define a medium K suite. These include abundant basalts and dacites, with a silica gap between 58 and 66 wt% SiO_2, suggesting that felsic magmas did not form by fractional crystallization of mantle-derived basalt. Phenocryst assemblages in mafic rocks show arc-like associations of anorthite-rich plagioclase with Fe-rich olivines. Magmatic temperatures calculated for coexisting ortho- and clinopyroxene indicate *c.* 1100 °C for a basaltic andesite and *c.* 800 °C for three dacites, typical for cool, wet, subduction-related felsic magmas. Low Sr/Y ratios indicate that felsic magma formed under low-P crustal conditions. Diamante cross-chain volcanoes mark a zone of along-arc (north) extension which focuses mantle melts into E–W magma-healed rifts, and leads to variable interaction with overlying crust. West Diamante Volcano lies on thin, refractory crust of the Mariana Trough back-arc basin so mantle-derived basalts erupt with little crustal interaction. In contrast, East Diamante is built on thickened arc crust with tonalitic middle crust that can be remobilized by basaltic intrusion. Once re-melted by mafic intrusions, this mid-crustal felsic reservoir could erupt because localization of north–south extension along the Diamante volcanic cross-chain facilitated the development of conduits to the surface.

Finally, the presence of at least seven, or perhaps eight volcanoes that erupt felsic magmas in a *c.* 115 km long arc segment called the 'Anatahan Felsic Province' indicate that a mid-crustal tonalite body exists beneath this part of the Mariana arc. Felsic eruptions can be expected anywhere in this region following intrusion of mafic magma at *c.* 1200 °C into thickened arc crust. The midcrustal tonalite layer can then be melted or remobilized at *c.* 800 °C and erupt.

NSF grant SGER-0909398 supported US involvement in NT0908 research cruise. NSF grant SGER-1026150 supported US involvement in NT1012 research cruise. Cook 7 expedition and sample investigation was supported by NSF grant OCE 0001827. We appreciate thoughtful reviews by Amy Draut and Karsten Haase. This is UTD Geosciences contribution #1243.

References

Allen, S. R. & McPhie, J. 2009. Products of Neptunian eruptions. *Geology*, **37**, 639–642.

Arculus, R. J. 2003. Use and abuse of the terms calcalkaline and calcalkalic. *Journal of Petrology*, **44**, 929–935.

Bachmann, O. & Bergantz, G. W. 2009. Rhyolites and their source mushes across tectonic settings. *Journal of Petrology*, **49**, 2277–2285.

Baker, E. T., Embley, R. W. *et al.* 2008. Hydrothermal activity and volcano distribution along the Mariana arc. *Journal of Geophysical Research, Solid Earth*, **113**, doi: http://dx.doi.org/10.1029/2007JB005423

Calvert, A. J., Klemperer, S. L., Takahashi, N. & Kerr, B. C. 2008. Three-dimensional crustal structure of the Mariana island arc from seismic tomography. *Journal of Geophysical Research*, **113**, B01406, doi: http://dx.doi.org/10.1029/2007JB004939

Castillo, P. R. 2006. An overview of adakite petrogenesis. *Chinese Science Bulletin*, **51**, 257–268.

Christiansen, E. H. 2005. Contrasting processes in silicic magma chambers: evidence from very large volume ignimbrites. *Geological Magazine*, **142**, 669–681.

Crawford, A. J., Falloon, T. J. & Eggins, S. 1987. Origin of island arc high-alumina basalts. *Contributions to Mineralogy and Petrology*, **97**, 417–430.

Dixon, T. H. & Stern, R. J. 1983. Petrology and geochemistry of submarine volcanoes in the Southern Mariana Arc. *Geological Society of America Bulletin*, **94**, 1159–1172.

Draut, A. E. & Clift, P. D. 2006. Sedimentary processes in modern and ancient oceanic arc settings: evidence from the Jurassic Talkeetna Formation of Alaska and the Mariana and Tonga arcs, Western Pacific. *Journal of Sedimentary Research*, **76**, 493–514.

Green, D. N., Evers, J. G., Fee, D., Matoza, R. S., Snellen, M., Smets, P. & Simons, D. 2013. Hydroacoustic, infrasonic and seismic monitoring of the submarine eruptive activity and sub-aerial plume generation at South Sarigan, May 2010. *Journal of Volcanology and Geothermal Research*, **257**, 31–43.

Heeszel, D. S., Wiens, D. A., Shore, P. J., Shiobara, H. & Sugioka, H., 2008. Earthquake evidence for along-arc extension in the Mariana Islands. *Geochemistry, Geophysics, Geosystems*, **9**, doi: http://dx.doi.org/10.1029/2008GC002186

Kato, T., Beavan, J., Matsushima, T., Kotake, Y., Camacho, J. T. & Nakao, S. 2003. Geodetic evidence of back-arc spreading in the Mariana Trough. *Geophysical Research Letters*, **30**, doi: http://dx.doi.org/10.1029/2002GL016757

Kelley, K. A., Plank, T., Newman, S., Stolper, E. M., Gove, T. L., Parman, S. & Hauri, E. H. 2010. Mantle melting as a function of water content beneath the Mariana Arc. *Journal of Petrology*, **51**, 1711–1738.

Lindsley, D. H. & Andersen, D. J. 1983. A two-pyroxene thermometer. Proceedings of 13th Lunar and Planetary Science Conference. *Journal of Geophysical Research*, **88**(Suppl.), 887–906.

Miyashiro, A. 1974. Volcanic rock series in island arcs and active continental margins. *American Journal of Science*, **274**, 321–355.

Nakajima, K. & Arima, M. 1998. Melting experiments on hydrous low-K tholeiite: implications for the genesis of tonalitic crust in the Izu–Bonin–Mariana arc. *The Island Arc*, **7**, 359–373.

Plank, T. & Langmuir, C. H. 1988. An evaluation of the global variations in the major element chemistry of arc basalts. *Earth and Planetary Science Letters*, **90**, 349–370H.

Shukuno, H., Tamura, Y., Tani, K., Chang, Q., Suzuki, T. & Fiske, R. S. 2006. Origin of silicic magmas and

the compositional gap at Sumisu submarine caldera, Izu–Bonin arc, Japan. *Journal of Volcanology and Geothermal Research* **156**, 187–216.

STEIGER, R. H. & JÄGER, E., 1977. Subcommision on Geochronology: convention on the use of decay constants in geo- and cosmochronology. *Earth and Planetary Science Letters*, **36**, 359–362.

STERN, R. J. 2010. The anatomy and ontogeny of modern intra-oceanic arc systems. *In*: KUSKY, T., MINGGUO, Z. & XIAO, W. (eds) *The Evolving Continents: Understanding Processes of Continental Growth*. Geological Society, London, Special Publications, **338**, 7–34.

STERN, R. J. & HARGROVE, U. S. 2003. The Anatahan Felsic Province in the Mariana Arc system. *EOS Transactions of the American Geophysical Union*, **84**, F1562 (abstract).

STERN, R. J., FOUCH, M. J. & KLEMPERER, S. 2003. An overview of the Izu–Bonin–Mariana subduction factory. *In*: EILER, J. & HIRSCHMANN, M. (eds) *Inside the Subduction Factory*, Geophysical Monograph, American Geophysical Union, Washington, DC, **138**, 175–222.

STERN, R. J., KOHUT, E. J., BLOOMER, S. H., LEYBOURNE, M., FOUCH, M. & VERVOORT, J. 2006. Subduction factory processes beneath the Guguan Cross-chain, Mariana Arc: no role for sediments, are serpentinites important? *Contributions to Mineralogy and Petrology*, **151**, 202–221.

STERN, R. J., TAMURA, Y. *ET AL.* 2008. Evolution of West Rota Volcano, an extinct submarine volcano in the Southern Mariana Arc: evidence from sea floor morphology, remotely operated vehicle observations and $^{40}Ar/^{39}Ar$ Geochronology. *The Island Arc*, **17**, 70–89.

STRAUB, S. M. 2008. Uniform processes of melt differentiation in the central Izu Bonin volcanic arc (NW Pacific). *In*: ANEN, C. & ZELLMER, G. F. (eds) *Dynamics of Crustal Magma Transfer, Storage and Differentiation*. Geological Society, London, Special Publications, **304**, 261–283.

SYRACUSE, E. M. & ABERS, G. A. 2006. Global compilations of variations in slab depth beneath arc volcanoes and implications. *Geochemistry, Geophysics, Geosystems*, **7**, doi: http://dx.doi.org/10.1029/2005GC001045

TAKAHASHI, N., KODAIRA, S., KLEMPERER, S., TATSUMI, Y., KANEDA, Y. & SUYEHIRO, K. 2007. Crustal structure and evolution of the Mariana intra-oceanic island arc. *Geology*, **35**, 203–206.

TAMURA, Y. & TATSUMI, Y. 2002. Remelting of an andesitic crust as a possible origin for rhyolitic magma in oceanic arcs: an example from the Izu–Bonin arc. *Journal of Petrology*, **43**, 1029–1047.

TAMURA, Y., TANI, K., ISHIZUKA, O., CHANG, Q., SHUKUNO, H. & FISKE, R. S. 2005. Are arc basalts dry, wet, or both? Evidence from the Sumisu Caldera volcano, Izu–Bonin Arc, Japan. *Journal of Petrology*, **46**, 1769–1803.

TAMURA, Y., ISHIZUKA, O. *ET AL.* 2010. Missing oligocene crust of the izu-bonin arc: consumed or rejuvenated during Collision? *Journal of Petrology*, **51**, 823–846.

TATSUMI, Y. & SUZUKI, T. 2009. Tholeiitic vs calc-alkalic differentiation and evolution of arc crust: constraints from melting experiments on a basalt from the Izu–Bonin–Mariana Arc. *Journal of Petrology*, **50**, 1575–1603.

WADE, J. A., PLANK, T. *ET AL.* 2005. The May 2003 eruption of Anatahan volcano, Mariana Islands: geochemical evolution of a silicic island-arc volcano. *Journal of Volcanology and Geothermal Research*, **146**, 139–170.

WOODHEAD, J. D. 1989. Geochemistry of the Mariana Arc (western Pacific). *Chemical Geology*, **76**, 1–24.

YORK, D. 1969. Least squares fitting of a straight line with correlated errors. *Earth and Planetary Science Letters*, **5**, 320–324.